Characteristics of Extracellular Potentials Recorded from the Sinoatrial Pacemaker of the Rabbit

MARVIN CRAMER, MICHAEL SIEGAL, J. THOMAS BIGGER, JR., AND BRIAN F. HOFFMAN

SUMMARY We have identified the extracellular potential changes associated with electrical activity of the sinoatrial (SA) pacemaker. Unipolar Ag-AgCl electrodes and DC amplification were used to record unipolar electrograms from the endocardial surface of the isolated rabbit atrium. Transmembrane action potentials (TAP) from the SA pacemaker were recorded to identify the pacemaker region and to monitor intracellular potential changes simultaneously with the electrogram. The SA electrogram showed two characteristic potentials when the electrode was in immediate proximity to pacemaking cells: (1) during phase 4 there was a steady slope (of the order of magnitude of −30 to −90 μV/sec at the cycle lengths studied) opposite in polarity to the slope of phase 4 of the TAP; (2) during the transition from phase 4 to phase 0 of the TAP the slope of the electrogram increased smoothly to approximately −400 to −800 μV/sec. We have called these two deflections the diastolic slope and the upstroke slope. As cells in the perinodal region and crista terminalis depolarized, these low frequency potential changes were interrupted by high frequency deflections. Tetrodotoxin (2–10 mg/liter) rendered the atrial muscle inexcitable and delayed and then abolished the high frequency activity in the SA electrogram, which then appeared as a continuous smooth tracing similar to the SA nodal TAP but reversed in polarity. The correlations between transmembrane and extracellular records were maintained when sinus automaticity was suppressed by cooling (36.5°C to 30°C). A potential resulting from pacemaker depolarization also could be recognized when the SA node was depolarized in a retrograde fashion by a paced atrial rhythm. These results demonstrate that rabbit SA pacemaker cells produce detectable and characteristic extracellular potential changes.

A NUMBER of significant disturbances of cardiac rhythm may result from abnormal electrical activity in and around the sinoatrial (SA) pacemaker.[1,2] To evaluate the state and function of the SA node, some investigators have developed indirect methods of estimating the velocity of impulse propagation into and out of the SA node region by measuring intervals between atrial responses to appropriately timed stimuli.[3,4] Others have used the extent to which overdrive prolongs the sinus cycle as an index of automaticity and conduction within the SA nodal region.[4,5] However, information derived from recordings of the transmembrane action potentials (TAP) of cells of the rabbit SA node[6] suggests that several of the assumptions on which the indirect techniques are based, such as the equality of conduction times into and out of the node, may not be correct. Clearly an extracellular record that identified and characterized the electrical activity of the SA pacemaker would have great potential for clinical research in this area.

Investigators have tried to identify an extracellular potential change characteristic of the electrical activity of the cardiac pacemaker ever since physiologists agreed that the rhythmic firing of the vertebrate heart is a consequence of some property of cardiac tissue and not the result of excitation by nerve impulses.[7] Early attempts to record the activity of the SA node from the canine heart through unipolar electrodes demonstrated a slow potential change which preceded the onset of atrial activation.[8] Bozler's studies on the hearts of amphibia demonstrated both slow oscillatory[9] and monotonic[10] potential changes that preceded the beginning of propagated activity. Rijlant[11] and Van der Kooi et al.[12] used closely spaced bipolar leads and recorded a signal composed predominantly of polyphasic high frequency components. More recently, Ramlau[13] used chronically implanted unipolar leads and recorded both slow and fast transients which appeared to precede the beginning of the P wave. However, proof that any of these potentials resulted from the electrical activity of automatic cells in the SA pacemaker was lacking. As a result, over the years electrophysiologists and cardiologists have relied on the demonstration of primary (or initial) negativity by the methods developed by Wybauw[14] and Lewis[15] to identify the approximate location of the SA pacemaker.

The characteristic TAP of normal cardiac pacemakers was described by Draper and Weidman[16] and West.[17] Their results, and those of others,[18–20] demonstrated characteristics of the TAP of the SA node which might give rise to unique extracellular potential changes. Automatic cardiac cells or fibers undergo slow depolarization during diastole (phase 4). Also, there is a gradual transition between the slow depolarization of phase 4 and the more rapid depolarization of phase 0. Although this second aspect of the transmembrane potential of an automatic cell is not uniquely related to normal automaticity, and can result from electrotonic interaction or very slow propagation, it is characteristic of the automatic cell. Fi-

From the Departments of Pharmacology and Medicine, College of Physicians and Surgeons, Columbia University, New York, New York.

Supported by a grant-in-aid, HE-08508-13, and by Program Project Grant HL-12738-08 from the National Heart and Lung Institute, National Institutes of Health. Dr. Cramer was a Cardiology Fellow supported by HL-05864. Dr. Siegal was an M.D.-Ph.D. candidate supported by GM-02042.

Address for reprints: Brian F. Hoffman, M.D., Department of Pharmacology, College of Physicians and Surgeons, 630 West 168th Street, New York, New York 10032.

Received August 9, 1976: accepted for publication January 27, 1977.

Downloaded from http://ahajournals.org by on March 4, 2022

nally, at least in the SA node, the slow depolarization during phase 4 is probably not a propagated change.[6, 19-23] Rather, many adjacent cells undergo slow depolarization that is similar in magnitude and more or less simultaneous; the potential change thus is analogous to a uniform "membrane"[20] rather than to a propagated action potential.

Recently Masuda and Paes de Carvalho[21] recorded transmembrane potentials and extracellular electrograms simultaneously to map the extracellular potentials generated in and around the SA nodal region of an isolated preparation of rabbit heart. Their results provide convincing evidence that the complex, high frequency deflections seen in electrograms from the SA node region are not due to depolarization of the pacemaker. Rather, they coincide with propagated depolarization of cells in the perinodal region and crista terminalis and occur 20-40 msec after inscription of phase 0 of the TAP of the pacemaker cells. In these same studies they concluded that activity of the pacemaker cells gave rise to no characteristic signal in the unipolar or bipolar electrogram.

We have used unipolar recording through Ag-AgCl electrodes and very high, direct-coupled amplification to study isolated preparations of rabbit SA node and canine Purkinje fibers. We believe we have recorded extracellular potentials produced by membrane currents of pacemaker cells. This paper describes the characteristics of the records we have obtained and our evidence that, through the use of appropriate methods, one can record an extracellular electrogram that is truly representative of the electrical activity of the SA pacemaker.

Methods

PREPARATIONS

Albino rabbits were killed by a blow on the occiput. The heart was rapidly removed through a median sternotomy and immersed in cool modified Tyrode's solution. Tissue containing the SA pacemaker cells and adjacent segments of the crista terminalis and atrial appendage was dissected free from the remainder of the heart and mounted with the endocardial surface uppermost in a tissue bath. The methods used have been described previously.[19] For most experiments the preparation was allowed to beat spontaneously during superfusion with Tyrode's solution warmed to 36-37°C, saturated with 95% O_2 and 5% CO_2, and pumped to the tissue bath at a rate of 12-15 ml/min. The composition of the Tyrode's solution (mM) was: NaCl, 137; KCl, 2.7; $CaCl_2$, 2.7; $NaHCO_3$, 12; $MgCl_2$, 0.5; glucose 5:5; NaH_2PO_4, 1.8.

Purkinje fibers were obtained from the right and left ventricles of mongrel dogs anesthetized with sodium pentobarbital (30 mg/kg, iv). The heart was removed through an incision between the right 4th and 5th ribs and immersed in cold Tyrode's solution. Bundles of Purkinje fibers were removed as the false tendons of the right and left ventricles and placed in the tissue bath and superfused in a manner similar to the preparation of rabbit atrium.

For some experiments (see Results, IIB and IID) the preparations were stimulated at a regular rate through fine Teflon-coated bipolar silver electrodes. Stimuli were isolated from ground and generated by a series of digital timers, counters, and pulse generators. For some experiments we made changes in the composition of the Tyrode's solution; these are described in Results. For other experiments drugs were added to the reservoir of Tyrode's solution perfusing the tissue. The agents used were tetrodotoxin (TTX) (Sigma), 2-10 mg/liter, and *dl*-isoproterenol (Winthrop), 10^{-8} to 10^{-6} M.

RECORDING TECHNIQUES

The methods used to record the TAP have been described previously.[19] Microelectrodes filled with 3 M KCl were coupled to amplifiers with high input impedance and input capacity neutralization through Ag-AgCl junctions. A ramp signal of 100 mV and 0.5-msec duration was injected between the bath and ground to calibrate the gain and frequency response of these amplifiers.

To record extracellular potential changes associated with pacemaker activity we used carefully matched Ag-AgCl leads 0.5 mm in diameter, covered to the tip with polyethylene and direct-coupled to a Tektronix 3 A9 preamplifier. Because, at the amplifications employed, high frequency deflections caused by atrial activation were off-scale, the upper frequency response of the amplifier was limited to 0.3 kHz. The electrodes were chlorided before each experiment and checked carefully to minimize liquid junction potentials and drift. With electrodes smaller in diameter some drift of the DC level was apparent and AC interference was greater. Electrodes were immersed in normal saline or Tyrode's solution at all times. The amplifier was virtually free of drift at a gain of 100 or 50 μV/cm. A "unipolar" recording mode was employed. For most experiments the indifferent electrode was located at the periphery of the tissue bath, 3 cm from the active electrode. The record of extracellular potential change was calibrated by signals of 50-100 μV delivered by a separate calibrator.

Both the intracellular microelectrodes and the unipolar extracellular electrode were mounted in micromanipulators and positioned over the tissue with the help of a binocular dissecting microscope. The extracellular unipolar electrode was placed about 0.2-0.5 mm above the preparation and the microelectrode mounted at an angle so that it could be advanced under the edge of the extracellular electrode to record from cells immediately subjacent to the extracellular electrode (Fig. 1). For some experiments a pair of Teflon-coated silver wires, 0.1 mm in diameter, was used to record a bipolar electrogram from atrial muscle. This record provided a time reference. All records were displayed on a Tektronix 565 oscilloscope and photographed with a Polaroid camera or recorded directly on a Gould Brush recorder at paper speeds of 5-50 mm/sec.

THE TISSUE CHAMBER

To minimize AC interference, the tissue bath was isolated from the perfusate by allowing the Tyrode's solution to drip into a receiving chamber. DC shifts associated with motion of the fluid surface were minimized by designing

Downloaded from http://ahajournals.org by on March 4, 2022

the tissue bath so that openings for the inflow and outflow of perfusate were below the surface (Fig. 1). The system was free of drift at a gain of 50 μV/cm.

OTHER TECHNIQUES

For some experiments, when all data had been recorded, we used the unipolar lead to obtain a record of an "injury potential" from the pacemaker region. This was accomplished by positioning the unipolar lead over the selected part of the preparation, recording the electrogram, and then pressing the electrode into the preparation using the coarse control of the micromanipulator.

Results

I. CHARACTERISTICS OF THE ELECTROGRAM AND LOCALIZATION OF THE PACEMAKER

Initially, the morphology and timing of the TAP of the SA node were used to locate the primary pacemaking area. Figure 2 shows a TAP recorded from a pacemaker cell and a direct-coupled extracellular electrogram recorded at high gain from the same site. The bottom record is a distant bipolar atrial electrogram that serves as a time reference. To facilitate comparison between the electrogram and TAP the polarity of the extracellular electrogram is reversed from the usual convention. The exploring electrode was connected to the negative terminal of the differential amplifier and thus a wave of depolarization approaching the exploring electrode yielded a negative (downward) deflection. It can be seen that there is a relationship between the extracellular and intracellular potentials recorded in the primary pacemaking area. During phase 4 of the TAP a steady "diastolic slope" (−40 μV/sec for this preparation) is recorded in the external unipolar electrogram. As the TAP shows the transition from phase 4 to phase 0, the external potential shifts to a much steeper "upstroke slope" (−450 μV/sec for this preparation). The smooth contour of the upstroke slope then is interrupted by high frequency deflections as cells outside the primary pacemaker are depolarized. These deflections appear to be superimposed on a slower change in potential that follows a voltage-time course similar to the repolarization of the TAP. This will be commented on subsequently. Extracellular electrograms showing *both* the slow diastolic change in potential and a smooth transition to an upstroke slope were not recorded from areas of the preparation other than that of the primary pacemaker. Two points should be emphasized. First, the slow diastolic and upstroke slopes showed precise temporal correlation with phases 4 and 0 of the transmembrane potential, and second, the upstroke slope preceded all high frequency activity. After the initial few experiments we routinely located the primary pacemaker by recording these characteristic potential changes in the electrogram.

Figure 3 shows records from several other sites in the same preparation. For each location records of extracellular electrogram and TAP are shown and the distal atrial electrogram continues to serve as a time reference. Figure 3A shows the same electrogram as Figure 2 but recorded at a slower sweep speed. Figure 3B shows TAP and surface recordings from a site midway between the primary

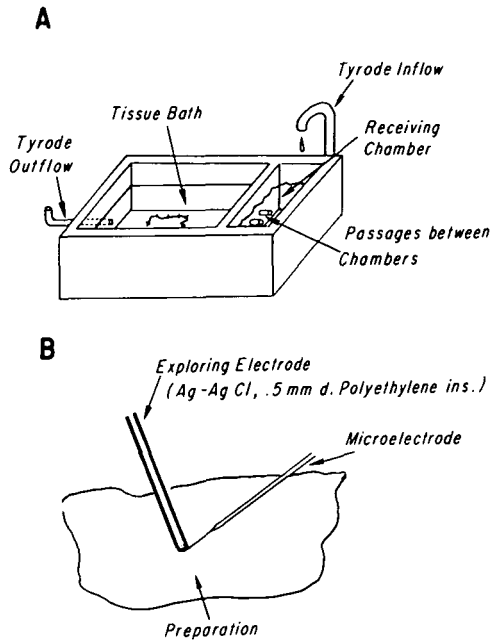

FIGURE 1 *A: diagram of the tissue chamber and the arrangements for electrical isolation from the source of perfusate, isolation of the tissue chamber from the chamber receiving the perfusate, and inlet and outlet ports below the surface of the fluid in the tissue chamber. B: the spatial relationships between the extracellular electrode and tissue surface that permitted the microelectrode to be inserted in a cell just beneath the tip of the extracellular electrode.*

pacemaker and the crista terminalis. Marked diastolic depolarization still is present in the TAP and a corresponding change in diastolic potential is evident in the extracellular recording. However, the transition from phase 4 to phase 0 is abrupt in both recordings and depolarization in this area occurs 30 msec after phase 0 of the TAP of the true

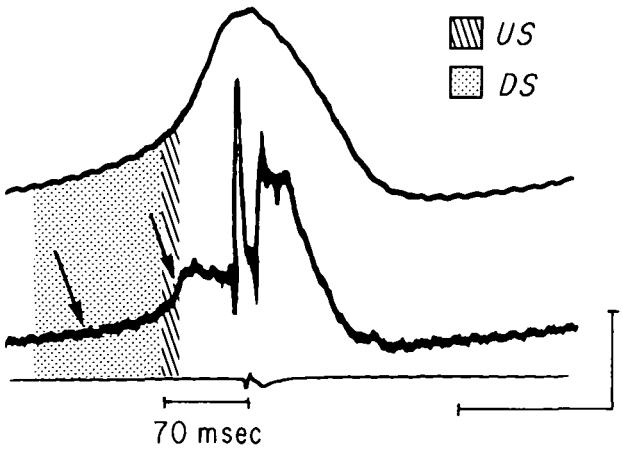

FIGURE 2 *Transmembrane potential (top trace) and unipolar extracellular electrogram (middle trace) from the primary pacemaking area recorded simultaneously with a bipolar atrial electrogram (bottom trace). Diastolic slope (DS) and upstroke slope (US) are indicated by arrows. DS is within the stippled area and US is within the area indicated by diagonal lines. Horizontal bar is 150 msec and vertical bar corresponds to 35 mV for the transmembrane record and 25 μV for the unipolar electrogram. High frequency components of the electrogram have been retouched for clarity.*

Downloaded from http://ahajournals.org by on March 4, 2022

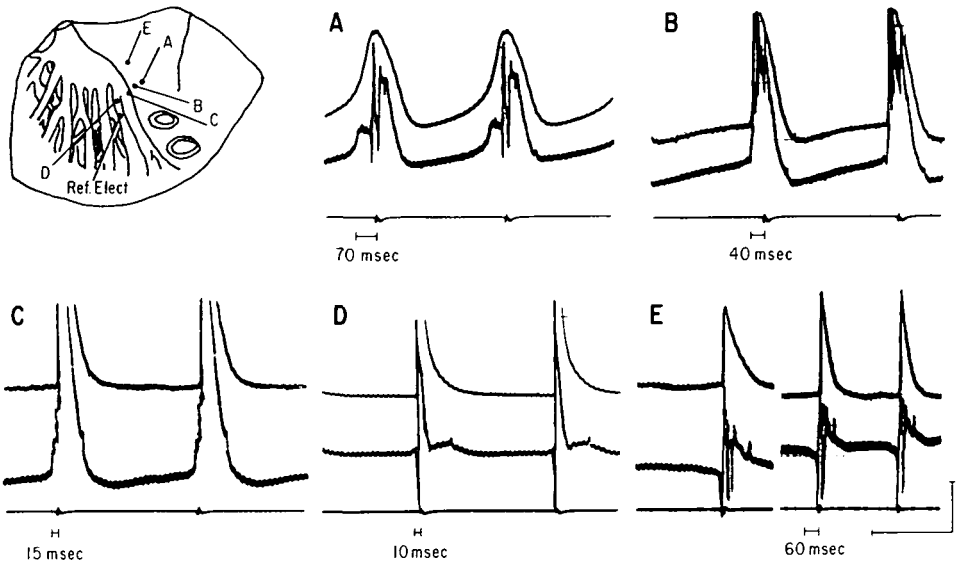

FIGURE 3 *Transmembrane potentials (upper trace) and extracellular electrograms (middle trace) recorded from several locations at and around the sinoatrial pacemaker as shown in the drawing of the preparation and each recording site. The bipolar atrial electrogram (bottom trace) was recorded from the same site throughout the experiment and serves as a time reference. Panel E is also shown at half sweep speed to emphasize slow potential changes below the baseline. The peak deflections of some transmembrane records (B-E) and high frequency components of some electrograms (B-D) were too large to be recorded on the oscilloscope screen at the amplifications used. Horizontal bar is 300 msec and vertical bar corresponds to 35 mV for transmembrane records and 25 μV for the unipolar electrogram. Some high frequency components of the electrogram are retouched for clarity. See text for discussion of individual records.*

pacemaker. The slow upstroke slope in the surface electrogram that characteristically is associated with true pacemaker depolarization cannot be seen. For Figure 3C the electrodes were positioned at the edge of the crista terminalis. Although there is no phase 4 depolarization in the TAP recording at this site, a diminished diastolic slope still can be seen in the extracellular record. This type of extracellular potential typically was seen at junctions between cell groups which did and did not demonstrate spontaneous diastolic depolarization. Such diastolic potentials recorded in the electrogram from transitional areas are probably produced by current between cells which did and did not undergo diastolic depolarization. When recordings were obtained from atrial trabeculae distal to the crista terminalis (Fig. 3D) the extracellular electrogram, with the amplication employed, no longer showed a diastolic slope. The electrogram here shows a small, short initial positive deflection. This most likely is caused by currents engendered by propagated activity in cells distal from the SA node because, as shown by the temporal relationship to the atrial electrogram, the small positive deflection occurs late in relation to the initiation of atrial activation. We have not attempted the detailed maps of potential distribution around the preparation that would permit us to advance evidence in support of this assumption.

At sites within the vena cava, rostral and caudal to the primary pacemaking area, the extracellular potentials were more variable. Figure 3E was recorded approximately 3 mm rostral to the pacemaking area. The TAP in this area does not show phase 4 depolarization, and phase 0 depolarization in this cell occurs at the same time as the depolarization complex of the reference atrial electrogram, 70 msec after pacemaker depolarization. The extracellular electrogram does not demonstrate either a diastolic or an upstroke slope. The earliest extracellular potential change is a 10-μV deflection below the baseline that begins about 60 msec before cells under the electrode are depolarized. Figure 4 shows intracellular and extracellular potentials recorded 3 mm rostral to the pacemaking site in a different preparation. The TAP of cells from this area demonstrate phase 4 depolarization and a low velocity of phase 0 depolarization; nevertheless, these cells are not in the primary pacemaking area because they depolar-

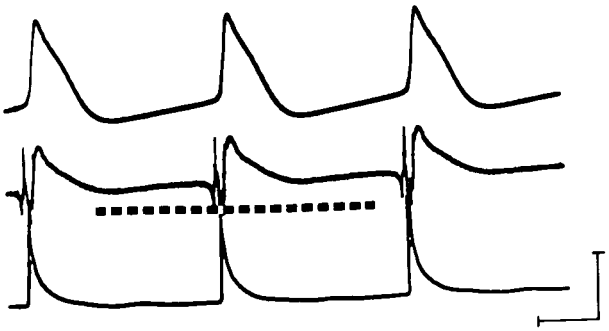

FIGURE 4 *Transmembrane potential (upper trace) and extracellular electrogram (middle trace) recorded from a site 2 mm rostral to the pacemaker. Atrial transmembrane potential (lower trace) serves as a time reference. Horizontal bar is 200 msec; vertical bar corresponds to 50 mV for the sinoatrial nodal transmembrane potential and 100 μV for the electrogram. High frequency components of extracellular electrogram are retouched for clarity. A dashed horizontal line is added to emphasize the slopes. See text for discussion.*

Downloaded from http://ahajournals.org by on March 4, 2022

ize after the reference TAP recorded from atrial muscle. The extracellular record at this site shows a diastolic slope but no upstroke can be detected. Instead, the extracellular record resembles that shown in Figure 3E: the diastolic slope is interrupted by an initial positive deflection which begins before cells under the electrode are depolarized. An upstroke slope is not seen because cells with rapid phase 0 upstroke velocities are depolarizing simultaneously, resulting in high frequency potentials which obscure the small low frequency waveforms. Potentials like those in Figures 3E and 4 were recorded from sites within the vein both rostral and caudal to the pacemaker. Since these changes in potential occur before the cells under the electrode undergo depolarization, are positive in sign and occur late in the atrial activation sequence, we believe they are caused by impulses propagating slowly from the pacemaking area towards extracellular electrode. Proof of this assumption would also require detailed mapping studies.

II. CONFIRMATORY EXPERIMENTS

To test our assumption that the diastolic and upstroke slopes are due to phase 4 and phase 0 depolarization of the pacemaker cells, respectively, we performed several additional types of experiments.

A. Effects of Tetrodotoxin

TTX blocks the fast Na^+ channel in many excitable tissues and, in concentrations of 1 mg/liter or higher, is reported to abolish electrical activity in the rabbit atrium without affecting that of the SA node.[22] We used TTX (2–10 mg/liter) to see whether the slow potentials in the surface electrogram would persist when electrical activity was restricted to the pacemaking area. Figure 5 shows the effects of TTX in such an experiment. Figure 5A is a control record and shows the external potential recorded over the pacemaking area with simultaneous TAP recordings from either the primary pacemaker or from an atrial trabecula. After beginning superfusion with TTX, conduction velocity slowed in the fast, Na^+-dependent tissues as shown in Figure 5B. Here, the extracellular tracing shows that the interval between the low frequency and high frequency activity in the electrogram has increased and the interval from the onset of the upstroke slope in the electrogram to atrial depolarization lengthens from 50 (Fig. 5A) to 110 (Fig. 5B) msec.

For Figure 5C the superfusion with TTX was continued and the delay between the upstroke slope and high frequency components of the electrogram lengthened until 2:1 block developed. As before, the external electrode was positioned over the primary pacemaker and the surface electrogram can be compared to TAP recordings from the primary pacemaker and the atrium. The extracellular slow potentials continue to show the same correlation with the TAP recordings as in the control records. High frequency activity in the electrogram occurs with every other beat and is related to depolarization of cells outside the pacemaker. For sinus beats that do not conduct out of the pacemaking area, the electrogram is a smooth, continuous tracing similar in shape to, but reversed in polarity from, the TAP recording. Once again there is a suggestive resemblance between the voltage-time course of the latter part of the electrogram and the repolarization phase of the TAP. This is commented on in the Discussion.

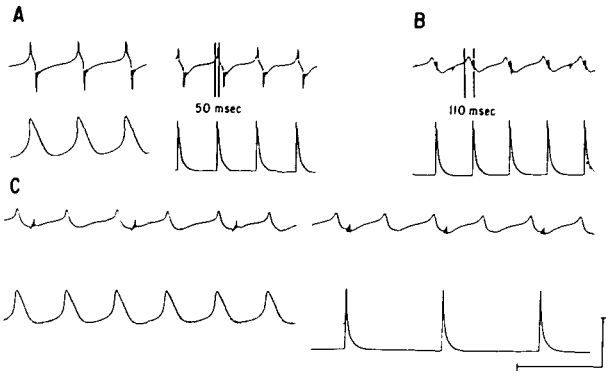

FIGURE 5 *Effects of tetrodotoxin (TTX) on the sinoatrial (SA) electrogram. Upper trace is an electrogram recorded at a fixed position over the SA pacemaker. Bottom traces are transmembrane potentials from either the SA pacemaker or an atrial trabecula. Horizontal bar is 1,000 msec and vertical bar corresponds to 100 mV for transmembrane potential and 200 μV for the electrogram. See text for discussion.*

Throughout the period of exposure to TTX the diastolic and upstroke slopes continued to show the same temporal correlations with phase 4 and phase 0 of the TAP as in the control records. Abolition of contraction of atrial muscle by TTX had no effect on the slow potential and thus it is not likely that it was due to movement. All effects of TTX were reversed on returning to perfusion with drug-free Tyrode's solution.

B. Extracellular Potentials Recorded from Purkinje Fibers Manifesting Spontaneous Phase 4 Depolarization

As a result of modification in ionic environment and of exposure to β-adrenergic agonists, canine cardiac Purkinje fibers develop spontaneous phase 4 depolarization that is comparable in magnitude to that of normally functioning SA node pacemaker cells. Under appropriate conditions such phase 4 depolarization of Purkinje fibers is a reasonably uniform phenomenon, i.e., the change in transmembrane potential occurs simultaneously throughout much or all of the preparation. This is readily demonstrated by recording transmembrane potentials at a number of sites in the fiber bundle. This phase 4 depolarization is analogous to that of the pacemaker area of the SA node. Therefore, we recorded extracellular electrograms from several preparations of canine Purkinje fibers induced to develop diastolic depolarization to determine whether such changes in their TAP were associated with detectable extracellular potential changes.

Transmembrane and extracellular recordings were obtained from Purkinje fibers initially perfused with Tyrode's solution in which K^+ = 4.0 mM and Ca^{2+} = 2.7 mM and then with solution in which K^+ was 1.3 and Ca^{2+} was 5.4 mM. After 30 minutes in the test solution isoproterenol was added to give a concentration of 10^{-8} to 10^{-6} M. Under control conditions (Fig. 6A) the TAP of the preparation showed no diastolic depolarization and the baseline of the extracellular electrogram showed no diastolic slope. After superfusion with low K^+, high $Ca2^+$ solution (Fig.

Downloaded from http://ahajournals.org by on March 4, 2022

6B), phase 4 depolarization of 30 mV/sec was seen in the TAP recorded from some cells and a corresponding extracellular potential (−30 μV/sec) was detected. After isoproterenol (10^{-6} M) had been added (Fig. 6C) the part of the preparation under the recording electrodes assumed an automatic rhythm that was completely dissociated from tissue depolarized by the stimulator (externally paced depolarizations are indicated by arrows) with all fibers showing uniform phase 4 depolarization. The spontaneous rhythm was more rapid than the paced rate and the slope of phase 4 depolarization in the TAP had increased (80 mV/sec). This increased phase 4 depolarization was reflected in the electrogram which showed a similar increase in diastolic potential (−60 μV/sec).

C. *Effects of Cooling*

We cooled rabbit sinus node preparations to evaluate the extent to which changes in the slope of phase 4 depolarization correlated with changes in the extracellular potentials. Figure 7 shows the effects of cooling the preparation from 36.5°C to 30°C while the positions of the surface electrode and microelectrode were held constant. The decrease in slope of phase 4 depolarization produced by cooling (30–10 mV/sec) was accompanied by a comparable decrease in the diastolic slope of the extracellular potential (−36 to 12 μV/sec). The upstroke slope continued to maintain a precise temporal relationship to phase 0 of the transmembrane action potential.

D. *Effects of Retrograde Depolarization of the Pacemaker on the Electrogram*

We also were interested in learning whether the pacemaker produced a recognizable extracellular potential when it was depolarized in a retrograde manner. Figure 8A shows the typical effects of a paced atrial rhythm on the extracellular electrogram of the primary pacemaker. The first depolarization originates in the primary pacemaker and the electrogram shows the slow upstroke slope from pacemaker cells preceding activity of crista terminalis and atrium. Subsequent complexes (indicated by arrows) are initiated by stimuli delivered to an atrial trabecula. As a result, the depolarization sequence in the SA nodal region is reversed and the electrogram shows high frequency potentials from the atrium, crista terminalis, and perinodal region preceding depolarization of the pacemaker. However, near the end of the high frequency potentials a slow wave also is recorded (indicated with dashed line in inset at the right). The onset of this slow potential is obscured by the preceding high frequency deflections but the peak and downslope appear to coincide with the peak and repolarization phase of the TAP of the pacemaker. To establish that this slow potential was due to depolarization of pacemaker cells and not to repolarization of atrial cells, we paced the preparation at rates fast enough to produce retrograde block of conduction into the pacemaking area. For Figure 8B the preparation was paced at a rate of 200 beats/min; this resulted in 3:2 conduction into the pacemaker. The first paced impulse conducted normally into the pacemaker, the second depolarized the pacemaker after a delay, and the third was blocked and did not elicit an action potential in the pace-

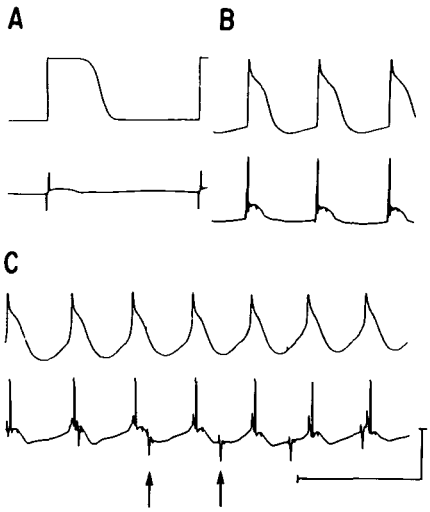

FIGURE 6 *Extracellular potential recorded from Purkinje fibers manifesting spontaneous phase 4 depolarization. In each figure the upper trace is a transmembrane potential and the lower record an extracellular electrogram from the same site. The peak of the action potential in panel A is off-scale. In panel C the part of the preparation under the electrode has assumed a spontaneous rhythm at a more rapid rate than the stimulus (externally paced beats indicated by arrows). Since these rhythms are completely dissociated, there must be conduction block between the paced part of the preparation and the area from which the records are obtained. Horizontal bar is 1,000 msec and vertical bar is 60 mV for the transmembrane record and 100 μV for the electrogram. See text for discussion.*

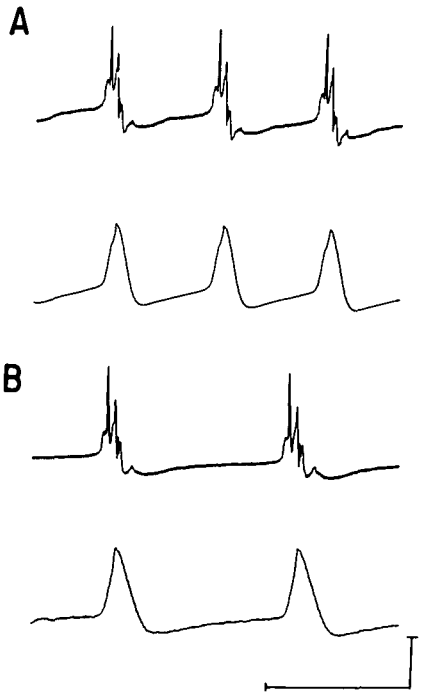

FIGURE 7 *Changes in extracellular (upper) and transmembrane (lower) records induced by cooling the preparation. The position of both the surface electrode and microelectrode was held constant. Horizontal bar is 1,000 msec and vertical bar corresponds to 40 mV for the transmembrane record and 50 μV for the electrogram. See text for discussion.*

Downloaded from http://ahajournals.org by on March 4, 2022

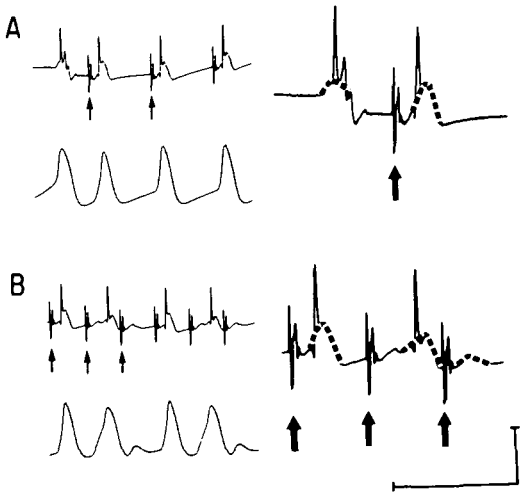

FIGURE 8 *Effects of retrograde depolarization of the pacemaker on the sinoatrial (SA) node electrogram. Upper traces are SA electrograms and lower traces transmembrane action potentials from pacemaker. In panel A the first action potential originates in the SA node and subsequent ones (arrows) are initiated by an external stimulus applied to an atrial trabeculum. All depolarizations in panel B are initiated by an external pacemaker at a rate of 200 and retrograde conduction into the SA pacemaker occurs in decremental fashion (3:2 Wenckebach). Insets at the right are enlarged 2.2× and show dashed lines drawn over the slow potentials for emphasis. Horizontal bar is 1,000 msec and vertical bar corresponds to 40 mV for transmembrane records and 100 μV for electrograms. See text for discussion.*

making cell. In every instance the low frequency extracellular potential reflected the change in TAP of the pacemaker, it was unchanged for the first impulse, delayed for the second, and greatly reduced for the third. Thus, pacemaker depolarization also is recognizable in the extracellular electrogram during retrograde activation of the pacemaker.

E. Injury Potential Produced by the Exploring Surface Electrode

To demonstrate that the microelectrode recording was representative of the TAP of most cells under the extracellular electrode, we ended some experiments by deliberately creating an injury potential with the extracellular electrode which was pressed into the surface of the tissue with the vertical control of the micromanipulator (Fig. 9). As cell membranes were traumatized and the surface electrode detected intracellular rather than an external potential, the polarity of the record reversed and its amplitude increased. The injury potential recorded in this way is analogous to the TAP recorded from the group of cells.

Discussion

We selected the rabbit SA node preparation as an experimental model to facilitate comparisons between simultaneous transmembrane and external potentials. The TAP characteristics and the spread of electrical activity within this preparation have been well characterized by previous investigators.[19, 23] The rabbit SA node is a sheet of cells that lies close to the intimal surface of the base of the

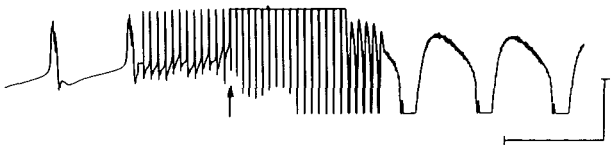

FIGURE 9 *Injury potential produced by pressing the surface electrode into the preparation. The first complexes are extracellular potentials recorded over the sinoatrial node pacemaker. The recording speed then was decreased from 50 cm/sec to 50 mm/sec and at the time indicated by arrow the surface electrode was pressed into surface of preparation. When the recording speed was returned to 50 cm/sec, the injury potential of pacemaker cells was seen. Vertical bar equals 100 μV. Horizontal bar is 1 second for the fast and 10 seconds for the slower recording speed. See text for further discussion.*

superior vena cava and shows regional differences in electrophysiological properties. The site in which the propagated impulse begins, the primary pacemaker, is an area no more than 1-2 mm in diameter which can be located almost anywhere in the base of the wall of the vein. The upstroke of the TAP of cells in the primary pacemaking area begins earlier than in any other cell group. Electrical activity in the primary pacemaker is characterized by prominent phase 4 depolarization and a smooth transition from phase 4 to the phase 0 upstroke. The depolarization wave spreads radially from the primary pacemaking area to activate the crista terminalis and other areas of the vena cava. Lesser degrees of diastolic depolarization also can be recorded in TAP from most of the other cells in the base of the superior vena cava, but the records from such "latent" pacemakers differ from those of primary pacemakers. The transition from phase 4 to phase 0 usually is more abrupt in latent pacemakers, and phase 0 upstroke velocity and amplitude may be greater in latent than in true pacemakers. It is clear from results of microelectrode studies that in order to record the onset of SA node activity through an extracellular electrode one must be able to detect an external potential produced by depolarization of the cells in the primary pacemaking area and distinguish it from signals caused by depolarization of large numbers of latent pacemaker cells.

Our results indicate that two low frequency, low voltage potential changes that we have recorded in proximity to the primary pacemaking area are produced by these cells. These components of the electrogram are: (1) the diastolic slope, a steady change in potential (−30 to 90 μV/sec) which occurs during the time the cells are undergoing phase 4 depolarization, and (2) the upstroke slope, another slow potential change (−400 to 800 μV/sec) which is produced by phase 0 depolarization of pacemaker cells. The unipolar electrograms sometimes appeared to demonstrate slow potentials with a voltage-time course similar to repolarization of the TAP of the subjacent cells (Fig. 2). These repolarization deflections were particularly obvious during retrograde depolarization deflections of the pacemaker, or after TTX had blocked activation of fibers with fast channels. However, these potentials were not seen in all electrograms (Fig. 5A), and because we did not conduct any systematic studies to identify the cause of this deflection we can do no more than comment on them.

Downloaded from http://ahajournals.org by on March 4, 2022

To understand how pacemaker cells give rise to the diastolic and upstroke slopes it is necessary to consider the relationship between extracellular and transmembrane potentials. Extracellular voltage changes in the vicinity of an electrically active tissue are due to the current crossing cell membranes and an associated current in the volume conductor surrounding the tissue. Since the volume conductor has inherent electrical resistance, the flow of current through it creates a potential field that varies in time as a function of the polarity and magnitude of the transmembrane current. Extracellular potentials associated with diastolic depolarization have not been reported previously; but such potentials must exist. When a cell undergoes spontaneous diastolic depolarization, the difference in transmembrane potential between it and adjacent, electrically coupled cells causes a current through the cell interiors, across the cell membrane, and along the extracellular conductors. This current is analogous to the "electrotonic current" associated with propagation and creates in the same manner a voltage gradient in the extracellular environment. If a sufficient number of closely grouped cells undergo phase 4 depolarization at the same time, as occurs normally in the SA node, the current passing across their membranes may well be strong enough to establish detectable potential gradients in the extracellular conductor.

Several lines of evidence support the idea that the gradual change in extracellular voltage during phase 4 is caused by membrane currents associated with diastolic depolarization. First, the slope can be recorded to a variable extent over the expanse of vein undergoing spontaneous phase 4 depolarization, but such a slope is not detected over tissues in which the transmembrane potential during phase 4 is constant (atrium or nonautomatic Purkinje fibers). In addition, the magnitude of the diastolic slope shows a correlation with the degree of phase 4 depolarization present in cells under the electrode. The external slope is greatest over and around the primary pacemaking area and is less prominent in other areas. As indicated in Figure 7, interventions which cause alterations in the slope of phase 4 depolarization produce similar changes in the diastolic slope recorded through an appropriately placed extracellular electrode. TTX, which abolishes all electrical activity outside the pacemaking area and renders the preparation motionless, has no effect on the diastolic slope in the electrogram or on the transmembrane potential of the SA pacemaker. Finally, when groups of Purkinje fibers are induced to develop marked diastolic depolarization, they generate extracellular potentials comparable to those recorded from the SA nodal pacemakers. All these results support the idea that nonpropagated phase 4 depolarization is associated with a transmembrane current or sufficient strength to produce detectable extracellular potentials.

The transmembrane currents associated with phase 0 depolarization of pacemaker cells initiate propagation of the impulse. We believe these currents are responsible for the upstroke slope. Studies of the relationship between the voltage detected by monopolar extracellular electrodes and that recorded with microelectrodes have been obtained during propagated activity in nerve, muscle, and Purkinje fibers.[24-26] These experiments have shown that the amplitude of the external potential may be related to the maximum rate of rise of phase 0, and that the duration of the external potential is related to phase 0 duration. Since we are monitoring the onset of propagation from a nonuniform sheet of cells rather than measuring propagated activity in the middle of a fiber which approximates an ideal cable, it probably is inappropriate to draw analogies between these studies and ours. However, despite such differences, these studies suggest that depolarization of pacemaker cells with their characteristically slow and prolonged phase 0 should give rise to a low amplitude slow potential such as is seen in the upstroke slope.

Evidence to support the argument that the upstroke slope is produced by membrane currents associated with true pacemaker depolarization is provided by our observation that the upstroke slope is found only over the primary pacemaking area and that the onset of the upstroke slope corresponds temporally to the onset of phase 0 depolarization of true pacemaker cells in transmembrane records. Further proof is provided by the experiments with TTX. During the superfusion with solution containing TTX the conduction velocity between pacemaker and atrium progressively slows until SA block is produced (Fig. 5B and C). However, the temporal relationship between the onset of phase 0 and the onset of the upstroke slope remains undisturbed. Thus, it is probable that the upstroke slope is produced by membrane currents associated with phase 0 and consequently is a reliable indicator of the onset of the action potential in the pacemaker.

A comparison of our electrograms with results of previous attempts to record from the sinus node with extracellular electrodes suggests that the low frequency potentials recorded by Bozler[9, 10] and Ramlau[13] may have been produced by depolarization of pacemaker cells. Bozler's records, which were obtained from strips of turtle sinus venosus by DC recording, demonstrate a slow potential similar in appearance to the upstroke slope (but several hundred microvolts in amplitude). The greater amplitude probably is due to his use of a steam bath, which increases the resistance of the volume conductor surrounding the tissue. Ramlau's electrograms were obtained through electrodes chronically implanted in dogs. Although he used a 2.05-Hz high band pass filter and his electrodes were 1.5 mm^2 in area, his records also show a low frequency potential similar to the upstroke slope. His experiments thus suggest that it may be possible to record sinus node electrograms from other species. It should also be noted that our results support those of Masuda and Paes de Carvalho[21] to the extent that we also found that high frequency deflections in the SA electrograms were produced by depolarization of perinodal and other cells in which phase 0 is rapid. The differences between their results and ours probably are due to our use of much higher DC amplification.

In addition to establishing that pacemaker cells give rise to recognizable extracellular potentials, we believe the current studies suggest how such potentials could be used to provide clinically relevant information. For example, the primary pacemaking site within the sinus node can be located without the aid of microelectrodes, and the time of pacemaker depolarization determined from the onset of

Downloaded from http://ahajournals.org by on March 4, 2022

the upstroke slope. Thus, SA conduction time can be measured directly. Furthermore, because depolarization of the pacemaker can be recognized during retrograde conduction, it probably is possible to determine the fastest paced rate at which retrograde conduction into the sinus node depolarizes the pacemaker in 1:1 fashion. This permits as evaluation of the refractoriness of tissues around the pacemaker and also allows a determination of the rate at which overdrive suppression of the pacemaker is maximal. This study demonstrates that rabbit sinus node pacemaker cells give rise to characteristic extracellular potentials. If similar slow potentials can be recorded from intact mammalian hearts, a highly informative procedure will become available for the study of sinus node physiology and pathophysiology.

References

1. Ferrer MI: Sick sinus syndrome in atrial disease. JAMA **206:** 645-651, 1968
2. Rubenstein JJ, Schulman CL, Yurchak PM: Clinical spectrum of the sick sinus syndrome. Circulation **46:** 5-13, 1972
3. Strauss, HC, Saroff AL, Bigger JT, Giardina EG: Premature stimulation as a key to the understanding of the sinoatrial conduction in man. Circulation **47:** 86-93, 1973
4. Mandel WJ, Laks MM, Obayashi K: Sinus node function. Arch Intern Med **135:** 388-394, 1975
5. Mandel WJ, Hayakawa H, Danzig R, et al: Evaluation of sino-atrial node function in man by overdrive suppression. Circulation **44:** 59-66, 1971
6. Miller S, Strauss HC: Measurement of sinoatrial conduction time by premature atrial stimulation in the rabbit. Circ Res **35:** 935-947, 1974
7. Erlanger J: The localization of impulse initiation and conduction in the heart. Harvey Lect 44-85, 1912-1913
8. Rilant R: La conduction dans le coeus du mammifere. Arch Int Physiol **33:** 325-496, 1931
9. Bozler E: The initiation of impulses in cardiac muscle. Am J Physiol **138:** 273-282, 1943
10. Bozler E: Tonus changes in cardiac muscle and their significance for the initiation of impulses. Am J Physiol **139:** 477-480, 1943
11. Rijlant P: Pacemaker of the mammalian heart. J Physiol (Lond) **75:** 28-29, 1932
12. Van der Kooi MW, Durrer RD, Van Dam RTH, Van der Tweel H: Electrical activity in sinus node and atrioventricular node. Am Heart J **51:** 684-700, 1956
13. Ramlau R: Electrograms of the sinoatrial node in dogs following surgical implantation of the sinoatrial node in dogs following surgical implantation of electrodes on the epicardium. J Electrocardiol **7:** 137-148, 1974
14. Wybauw R: Sur le point d'origine de la systole cardiaque dans l'oreillette drorte. Arch Int Physiol **10:** 78-90, 1910
15. Lewis T: Galvanometric curves yielded by cardiac beats generated in various areas of the auricular musculature; the pacemaker of the heart. Heart **2:** 23-46, 1910
16. Draper MH, Wiedman S: Cardiac resting and action potentials recorded with an intracellular electrode, J Physiol (Lond) **115:** 74-94, 1951
17. West TG: Ultramicroelectrode recording from the cardiac pacemaker. J Pharmacol Exp Ther **115:** 283-290, 1955
18. Brooks C McC, Lu HH: Sinoatrial Pacemaker of the Heart. Springfield, Ill., Charles C Thomas, 1972
19. Strauss HC, Bigger JT Jr: Electrophysiological properties of the rabbit sinoatrial perinodal fibers. Circ Res **31:** 490-506, 1972
20. Paes de Carvalho A, Hoffman BF, de Paula Carvalho M: Two components of the cardiac action potential. J Gen Physiol **54:** 607-635, 1969
21. Masuda MO, Paes de Carvalho A: Sinoatrial transmission and atrial invasion during normal sinus rhythm in the rabbit heart. Circ Res **37:** 414-421, 1975
22. Sano T, Yamagishi S, Iida Y: Several aspects on the spontaneous activity of the sinus node and its spread. Jap Circ J **30:** 134-138, 1966
23. Sano T, Yamagishi S: Spread of excitation from the sinus node. Circ Res **26:** 423-430, 1965
24. Lorente de Nó R: Analysis of the distribution of the action currents of nerves in volume conductors. Stud Rockefeller Inst Med Res **132:** 384-497, 1947
25. Hakansson GH: Action potentials recorded intra- and extracellularly from the isolated frog muscle fibre in Ringers solution and in air. Acta Physiol Scand **39:** 291-312, 1957
26. Spach MS, Barr RC, Serwer GA, Kootsey JM, Johnson EA: Extracellular potentials related to intracellular action potentials in the dog Purkinje system. Circ Res **30:** 505-519, 1972

Downloaded from http://ahajournals.org by on March 4, 2022